USASP
US ASSOCIATION FOR THE STUDY OF PAIN

PUBLISHED BY
ELSEVIER

The Journal of Pain, Vol 22, No 11 (November), 2021: pp 1385–1395
Available online at www.jpain.org and www.sciencedirect.com

Sensory Innervation of Human Bone: An Immunohistochemical Study to Further Understand Bone Pain

Jasper G. Steverink,[*,‡] Douwe Oostinga,[*] Floris R. van Tol,[*,‡] Mattie H.P. van Rijen,[*] Claire Mackaaij,[†] Suzanne A.M.W. Verlinde-Schellekens,[†] Bas J. Oosterman,[‡] Albert J.M. Van Wijck,[§] Tom A.P. Roeling,[†] and Jorrit-Jan Verlaan[*,‡]

[*]*Department of Orthopedic Surgery, University Medical Center Utrecht, The Netherlands,* [†]*Department of Anatomy, University Medical Center Utrecht, The Netherlands,* [‡]*SentryX B.V., Woudenbergseweg 41, Austerlitz, The Netherlands,* [§]*Department of Anesthesiology, University Medical Center Utrecht, The Netherlands*

Abstract: **Skeletal diseases and their surgical treatment induce severe pain. The innervation density of bone potentially explains the severe pain reported. Animal studies concluded that sensory myelinated Aδ-fibers and unmyelinated C-fibers are mainly responsible for conducting bone pain, and that the innervation density of these nerve fibers was highest in periosteum. However, literature regarding sensory innervation of human bone is scarce. This observational study aimed to quantify sensory nerve fiber density in periosteum, cortical bone, and bone marrow of axial and appendicular human bones using immunohistochemistry and confocal microscopy. Multivariate Poisson regression analysis demonstrated that the total number of sensory and sympathetic nerve fibers was highest in periosteum, followed by bone marrow, and cortical bone for all bones studied. Bone from thoracic vertebral bodies contained most sensory nerve fibers, followed by the upper extremity, lower extremity, and parietal neurocranium. The number of nerve fibers declined with age and did not differ between male and female specimens. Sensory nerve fibers were organized as a branched network throughout the periosteum. The current results provide an explanation for the severe pain accompanying skeletal disease, fracture, or surgery. Further, the results could provide more insight into mechanisms that generate and maintain skeletal pain and might aid in developing new treatment strategies.**

Perspective: ***This article presents the innervation of human bone and assesses the effect of age, gender, bone compartment and type of bone on innervation density. The presented data provide an explanation for the severity of bone pain arising from skeletal diseases and their surgical treatment.***

Key words: *Bone pain, innervation density, periosteum, cortex, bone marrow.*

Received February 26, 2021; Revised April 14, 2021; Accepted April 23, 2021.

Funding Sources: This research did not receive any specific grant from funding agencies in the public, commercial, or not-for-profit sectors.

Disclosures: J.G. Steverink, F.R. van Tol, B.J. Oosterman and J.J. Verlaan own stock in and are paid employees of SentryX B.V., Netherlands. These disclosures are unrelated to this study. D. Oostinga, M.H.P. van Rijen, C. Mackaaij, S.A.M.W. Verlinde-Schellekens, A.J.M. van Wijck, and T.A.P. Roeling report no conflicts of interest.

Address reprint requests to Jasper G. Steverink Department of Orthopedic Surgery, Heidelberglaan 100, 3584CX, Utrecht, Netherlands E-mail: J.G.Steverink-4@umcutrecht.nl

1526-5900/$36.00

https://doi.org/10.1016/j.jpain.2021.04.006

Musculoskeletal diseases are highly prevalent in the general population and are a leading cause of disability among patients and medical costs every year.[5,21,32,34,44,58] Diseases affecting bone and their (surgical) treatment can lead to considerable pain.[18] Bone pain negatively affects mobility, inhibits rehabilitation, and can lead to long-term disabilities.[12,13,42,50,53,62,63] The complex underlying mechanisms and multiple possible etiologies of bone pain, make this pain difficult to attenuate.[39,46,48]

A deeper understanding of sensory innervation of human bones could aid in improved treatment of bone

pain. Recent reports have shown innervation density to correlate with the presence of pain, for example regarding intervertebral disc innervation in low back pain.[15,43] However, literature on human bone innervation is scarce. Some early reports on human bone innervation exist, but these studies did not yet have access to current advanced imaging techniques.[49,61] Previous studies in rodents demonstrated that periosteum, cortical bone and bone marrow are all innervated with afferent sensory nerve fibers and post-ganglionic sympathetic neurons.[8,9,27,37,41,59] The main function of sensory nerve fibers is conduction of sensory stimuli from the bone, however, together with sympathetic fibers, they also play a role in bone healing and remodeling.[2,7,10,17,33,45,47,54] Several mammalian studies identified two important types of sensory nerve fibers performing these functions: myelinated A∂-fibers and smaller diameter, unmyelinated C-fibers.[8,23,24,26,27,38] A∂-fibers are mainly responsible for conducting sharp, localized pain, while C-fibers transmit dull, diffuse pain.[40] Earlier mammalian studies concluded that innervation density of sensory nerve fibers is highest in the periosteum, followed by bone marrow and cortical bone.[8,37] The periosteum is therefore suggested to be a major contributor to pain arising from musculoskeletal diseases, but data in humans are lacking.

The aim of the present study was to quantitatively explore the number and distribution of A∂-fibers, C-fibers, and sympathetic fibers in axial and appendicular human bones using immunohistochemistry, and fluorescent and confocal microscopy. Furthermore, this study set out to assess the distribution of nerve fibers between different bone-related compartments (ie periosteum, bone marrow, and cortical bone), between different anatomical locations (ie neurocranium, thoracic spine, upper extremity and lower extremity), and between genders. Lastly, the effect of age on bone innervation in the elderly population included in this study was determined.

Methods

Tissue Collection

In order to represent the human skeleton as completely as possible, experiments were performed on available anatomical specimens from parietal bones of the neurocranium, thoracic vertebral bodies, midshaft humeri, midshaft radii, midshaft femora, and midshaft tibiae. Of all bones, a cross-section containing periosteum, cortical bone and bone marrow was retrieved (Fig. 1). To prevent interference of joint disease in innervation density, midshaft portions of long bones were used.[6,28] No approval was needed from the medical research ethics committee for this study. Tissues were collected from bodies that entered the department of anatomy of our institution through a donation program. These persons provided written consent during life, that allowed the use of their entire bodies for educational and research purposes and therefore, samples were collected based on availability.

Bodies were previously fixated in 4% formaldehyde for varying durations (6 mo − 4 y). Age and sex of the bodies was known. From the long bones, 0.5 cm transversal sections of the diaphysis were gently cut using a saw (Dremel 3000, Racine, WI, USA), and from the thoracic vertebrae 0.5 cm sagittal sections of the vertebral body. Sections measuring 1 × 1 cm from the parietal bone of the neurocranium were obtained using a saw. The anatomical specimens were stored until further processing in 4% buffered formaldehyde to preserve tissue characteristics and prevent decay.

Tissue Processing

The collected anatomical specimens were decalcified using 0.5 M ethylenediaminetetraacetic acid (EDTA). Every seven days the decalcification progress was radiographically monitored using a μ-CT scanner (PerkinElmer Quantum FX, Waltham, MA, USA). After each cycle of seven days, anatomical specimens were again fixated with 4% formaldehyde overnight, and placed in fresh EDTA the next day. Upon complete decalcification, anatomical specimens were stored in 15% sucrose in 0.1 M phosphate-buffered saline (pH 7.4) at 4°C for further processing.

Anatomical specimens were dehydrated in graded ethanol series, cleared in xylene and embedded in paraffin. 5 μm thick sections were cut and mounted on clean, positively charged microscopic slides (VWR Premium Printer Slides, Radnor, PA, USA). Cross-sections were dried overnight at room temperature (RT), placed for five hours on a 60°C plate, and subsequently

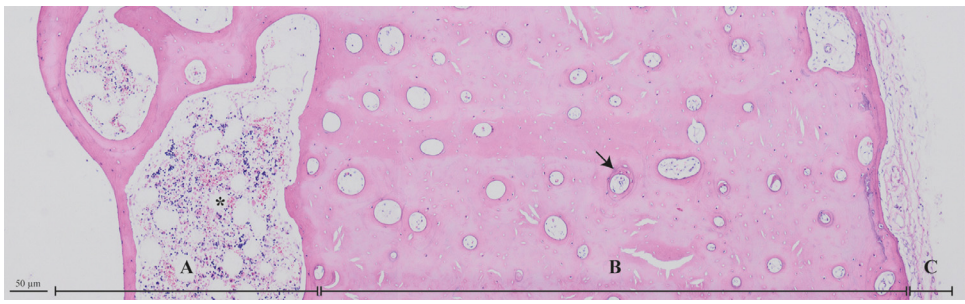

Figure 1. A cross-section of a radius stained with hematoxylin and eosin (H&E) displays the three bone-related compartments: bone marrow/trabecular bone (**A**), cortical bone (**B**) and periosteum (**C**) (50x magnification). The bone marrow consists of hematopoietic stem cells and adipose tissue (asterisk). In the cortical bone, Haversian canals run parallel to the longitudinal axis of the bone as part of an osteon and contain blood vessels and/or nerve fibers (arrow). The periosteum is a thin sheath of connective tissue that surrounds the outer surface of the cortical bone and consists of a cellular rich layer and a fibrous layer.

incubated at 60°C overnight to improve microscopic slide attachment.

Immunohistochemistry on Bone Cross-Sections

With immunohistochemistry, distinctive molecular markers can be used to label and visualize specific sensory and sympathetic nerve fibers. Aδ-fibers were labeled with anti-neurofilament 200 kD (NF-200) antibodies (Developmental Studies Hybridoma Bank, Iowa City, IA, USA). NF-200 is an intermediate filament part of the cytoskeleton of Aδ-fibers.[26,31] C-fibers express calcitonin gene-related peptide (CGRP), a neurotransmitter involved in nociception and nerve injury, and were labeled with anti-CGRP (Sigma-Aldrich, St. Louis, MO, USA).[11,26,56] Anti-tyrosine hydroxylase (TH) antibodies (Pel-Freez, Rogers, AR, USA), an enzyme part of the catecholamine synthesis, were used to label sympathetic fibers.[19] Anti-Protein gene product 9.5 (PGP9.5) (Dako, Carpinteria, CA, USA) antibodies were used as a pan-neuronal marker.[14,36,60] As positive controls, a human vagus nerve for NF-200, CGRP, PGP9.5 antibodies, and a human sympathetic trunk for TH and PGP9.5 antibodies were used. Primary antibodies were omitted in the negative controls. Details of the primary antibodies, including references to antibody characterization, are presented in Table 1.

Bone cross-sections were deparaffinized in xylene (3 × 5 min), stepwise hydrated in an ethanol gradient (3 × 5 min in 100% and in 96%, 3 min in 80%, 70%, and 50%), and subsequently washed in de-ionized water. For antigen retrieval, cross-sections were incubated in 0.01M citrate buffer (pH 6.0) for five minutes at RT. Samples were then transferred to an 80°C citrate buffer for 40 minutes, and subsequently cooled down to RT. Bone cross-sections were rinsed with wash buffer (0.05 M tris-buffered saline (TBS) (pH 7.6) and 0.05% Tween), and blocked with 5% normal human serum (Jackson Immuno Research, West Grove, PA, USA) in 0.05 M TBS (pH 7.6) for ten minutes at RT. The blocking buffer was removed, and primary antibodies were added in TBS with 3% bovine serum albumin (BSA) (GERBU Biotechnik GmbH, Heidelberg, BW, DE), and incubated overnight at 4°C, except for the PGP9.5 antibodies, which were applied for 48 hours.

Table 1. Background Information on Primary and Secondary Antibodies

Primary/secondary antibody	Immunogen	Manufacturer, species raised in, mono/polyclonal, catalogue and lot number	Dilution	Reference
PGP9.5	Purified PGP9.5 isolated from bovine brain	Dako, rabbit, polyclonal, Cat# Z5116, Lot# 20043529	Cross-sections: 1:2000 Whole-mount: 1:100	Manufacturer's information (Bernal Sierra et al., 2017)[3] (Cleypool et al., 2020)[12] (Rots et al., 2019)[51]
NF-200	Semi-purified neurofilament 200 kD from rat brain homogenate	Developmental Studies Hybridoma Bank (DSHB), mouse, monoclonal, Cat# RT97	Cross-sections: 1:1000	Manufacturer's information (Haskins et al., 2017)[20] (Lawson et al., 1993)[30] (Viehöfer et al., 2015)[62]
CGRP	Purified rat α-CGRP peptide. The epitope recognized by the antibody resides within the C-terminal ten amino acids of rat α-CGRP	Sigma-Aldrich, mouse, monoclonal, Cat# C7113, Lot# 106M4836V	Cross-sections: 1:500	Manufacturer's information (Yen et al., 2006)[65]
TH	SDS-denatured rat tyrosine hydroxylase purified from pheochromocytoma	Pel-Freez, rabbit, polyclonal, Cat# P40101, Lot# AJO319O	Cross-sections: 1:500 Whole-mount: 1:100	Manufacturer's information (Cleypool et al., 2020)[12] (Rots et al., 2019)[51]
BrightVision Poly-AP Anti-rabbit		ImmunoLogic (VWR), goat, Cat# VWRKDPVM110AP, Lot# 191217	Used for cross-sections	
BrightVision Poly-AP Anti-mouse		ImmunoLogic (VWR), goat, Cat# VWRKDPVR110AP, Lot# 251018	Used for cross-sections	
Alexa Fluor 594 Goat Anti-rabbit		Jackson ImmunoResearch, goat, polyclonal, Cat# 111-586-045, Lot# 112163	Whole-mount: 1:200	

After incubation in primary antiserum, bone cross-sections were washed with wash buffer, followed by incubation in secondary antibodies for 30 minutes at RT. BrightVision Poly AP-anti-Rabbit (ImmunoLogic VWR, Amsterdam, NH, NL) was used for TH and PGP 9.5 antibodies, and Poly AP-anti-Mouse for NF-200 and CGRP antibodies. Bone cross-sections were then rinsed with wash buffer, followed by 10 minutes incubation in Liquid Permanent Red (LPR) (Dako, Carpinteria, CA, USA). LPR was washed away with TBS and de-ionized water. To obtain sufficient contrast for tissue examinations, bone cross-sections were counterstained with hematoxylin. Finally, a cover slip with Entellan (Merck KGaA, Darmstadt, HE, DE) was applied, and bone cross-sections were air dried for 12 hours at RT before imaging.

Immunohistochemistry on Whole-Mount Preparations of Periosteum

Whole-mount preparations of periosteum were harvested from midshaft radii. Excess muscle was removed using a carbon steel surgical blade No. 20 (Swan-Morton, Sheffield, YSS, ENG). Sharpey's fibers were gently cut, and periosteum was taken off the bone by careful elevation. The periosteum was constantly irrigated with TBS during dissection to prevent tissue dehydration. Whole-mount samples were then frozen and thawed twice in TBS, and washed in whole-mount wash buffer (0.05 M TBS (pH 7.6) and 0.1% Saponin). Subsequently, whole-mount samples were incubated for 90 minutes at 37°C in blocking solution containing 5% normal human serum and whole-mount wash buffer. Primary antibodies TH and PGP9.5 were applied for 12 hours and 48 hours, respectively, in whole-mount wash buffer with 3% BSA at RT. Primary antiserum was aspirated and whole-mount samples were rinsed with whole-mount wash buffer. Alexa Fluor 594 goat anti-rabbit secondary antibodies (Jackson ImmunoResearch, West Grove, PA, USA) were applied for 30 minutes at RT in whole-mount wash buffer. BSA (3%) was added to minimize non-specific binding. Finally, samples were washed with whole-mount wash buffer, covered with FluorSave (Sigma-Aldrich, St. Louis, MO, USA), and dried for 12 hours at RT before imaging.

Microscopy and Nerve Fiber Quantification

High-power field (HPF, 400x magnification) images of bone cross-sections were captured with a Leica DM6 B (Wetzlar, HE, DE) fluorescent microscope using LAS X imaging software. A 400x magnification (311 $\times$ 233 μm in dimension) was used to distinguish between individual axons. The I3 filter cube (excitation range: blue, excitation filter: BP 450 - 490 nm, dichromatic mirror: 510 nm, and suppression filter: LP 515 nm) was set. Three HPFs were obtained per bone compartment per histology slide. The imaging location was chosen so that each set of three HPFs would adequately resemble the overall bone-related compartment. Fluorescent images of bone cross-sections were analyzed, and nerve fibers were quantified manually in ImageJ (NIH, Bethesda, MD, USA) by two observers (J.S. and D.O.). A fiber was counted if it was identifiable as a vividly fluorescent solid, solitary, round (in case of transverse cross-section) or elongated (in case of longitudinal cross-section) structure. No minimal dimensions were pre-specified. In case one fiber yielded more than one cross-section due to a sinuous course, this was counted as a single fiber. Mean fiber count of the three HPFs and of both observations was used for analysis. Brightness and contrast were adjusted to enhance image quality, no other image corrections or filters were used.

For whole-mount preparations of periosteum, images were captured with a ZEISS LSM 800 (Oberkochen, BW, DE) laser confocal microscope using a 5x objective, a 180 μm pinhole and ZEN imaging software. A 594 nm excitation beam was used, and emission was detected using a 620 nm emission filter. Z-stacks were generated to allow for three-dimensional assessment of nerve fiber distribution through the full-thickness periosteum using a 25 μm step size. Acquired images of whole-mount preparations were displayed as a maximal intensity projection in ImageJ. Background was subtracted using the Subtract Background function in ImageJ, and brightness and contrast were adjusted in Adobe Photoshop (Adobe Systems Incorporated, San Jose, CA, USA).

Statistical Analysis

Data was subsequently analyzed in RStudio version 1.2.5033 (RStudio Inc., Boston, MA, USA). Data distribution was checked for normality graphically, using Q-Q plots, and confirmed using Shapiro-Wilk testing. Spearman's Rho and an Intra-Class Correlation coefficient for absolute agreement were calculated to assess inter-observer variation. Comparisons were performed using a Kruskal-Wallis test and a post hoc Wilcoxon rank-sum test. P-values were corrected for multiple testing with a Bonferroni correction. A multivariate regression was performed using a generalized linear model with Poisson residuals and a log link function allowing for identification of interaction effects between variables. Residuals were checked for normality using Q-Q plots. If interaction effects were statistically significant, the effect was embedded into the generalized linear model. Variables studied were age, gender, bone-related compartment (ie periosteum, bone marrow, and cortical bone), immunohistochemical staining, anatomical location, and nerve fiber count. As nerve fiber count functioned as the outcome variable, ten unique interaction effects were possible and thus analyzed. Data were presented as median number of nerve fibers with interquartile range (IQR). Results from the multivariate regression were reported as incident rate ratios (IRR) calculated from Poisson coefficients ($e^{\text{Poisson coefficient}}$), and represent a multiplicative factor. In addition, estimated marginal means (EMM) with standard error (SE) were presented. The level of significance was set at $P < .05$.

Results

Demographics of Collected Tissue

A total of 54 anatomical specimens were harvested from 29 human fixated cadavers. Four parietal bones (7%), six thoracic vertebrae (11%), five midshaft humeri (9%), seven midshaft radii (13%), 17 midshaft femora (32%), and 15 midshaft tibiae (28%) were available and studied after harvesting. Sixteen (55%) cadavers were female, and overall mean age was 84.0 ± 8.2 years (range 66–99). Anatomical specimen characteristics are displayed in Table 2. Complete decalcification of anatomical specimens was achieved after a maximum of 23 days. A total of 3 NF-200, 5 CGRP, 4 TH, and 1 PGP9.5-stained bone cross-sections failed during the immunohistochemical staining process and were thus discarded, despite protocol changes to improve microscopic slide attachment.

Innervation of the Periosteum, Cortical Bone, and Bone Marrow

Overall, periosteum contained most nerve fibers, as compared to bone marrow, and cortical bone (Fig 2). The amount of Aϑ-fibers was largest in the periosteum (median 7 (IQR 4–12) fibers/HPF; $P < .001$ versus cortical bone, $P < .001$ versus bone marrow), followed by bone marrow (2 (1–4) fibers/HPF; $P < .001$ vs cortical bone), and cortical bone (0 (0–1) fibers/HPF) (Fig2A1-A3, E). The number of C-fibers in periosteum was higher (6 (3–10) fibers/HPF; $P < .001$ vs cortical bone, $P = .075$ vs bone marrow), compared with bone marrow (5 (2.75–8) fibers/HPF; $P < .001$ vs cortical bone), and cortical bone (1 (1–2) fibers/HPF) (Fig 2B1-B3,2E). The number of sympathetic nerve fibers was greatest in periosteum (9 (6–13) fibers/HPF; $P < .001$ vs cortical bone, $P < .001$ vs bone marrow), followed by bone marrow (5 (3–9) fibers/HPF; $P < .001$ vs cortical bone), and cortical bone (2 (1–4) fibers/HPF) (Fig 2C1-C3, E). PGP9.5-positive nerve fibers were mostly present in periosteum (9 (6–16.2) fibers/HPF; $P < .001$ vs cortical bone, $P < .001$ vs bone marrow), followed by bone marrow (3 (2–5.75) fibers/HPF; $P < .001$ vs cortical bone), and cortical bone (1 (1–3) fibers/HPF) (Fig 2D1-D3, 2E). Spearman's Rho was 0.890 and the intra-class correlation coefficient for absolute agreement was 0.851 (0.751–0.904), indicating good to excellent agreement between observers.[29,55]

Table 2. Bone Sample Characteristics

Characteristics	Value
Gender, n (%)	
Female	16 (55%)
Male	13 (45%)
Age, mean (SD) (years)	84.0 (±8.2)
Bones, n (%)	N = 54
Neurocranium	4 (7%)
Thoracic vertebra	6 (11%)
Midshaft humerus	5 (9%)
Midshaft radius	7 (13%)
Midshaft femur	17 (32%)
Midshaft tibia	15 (28%)

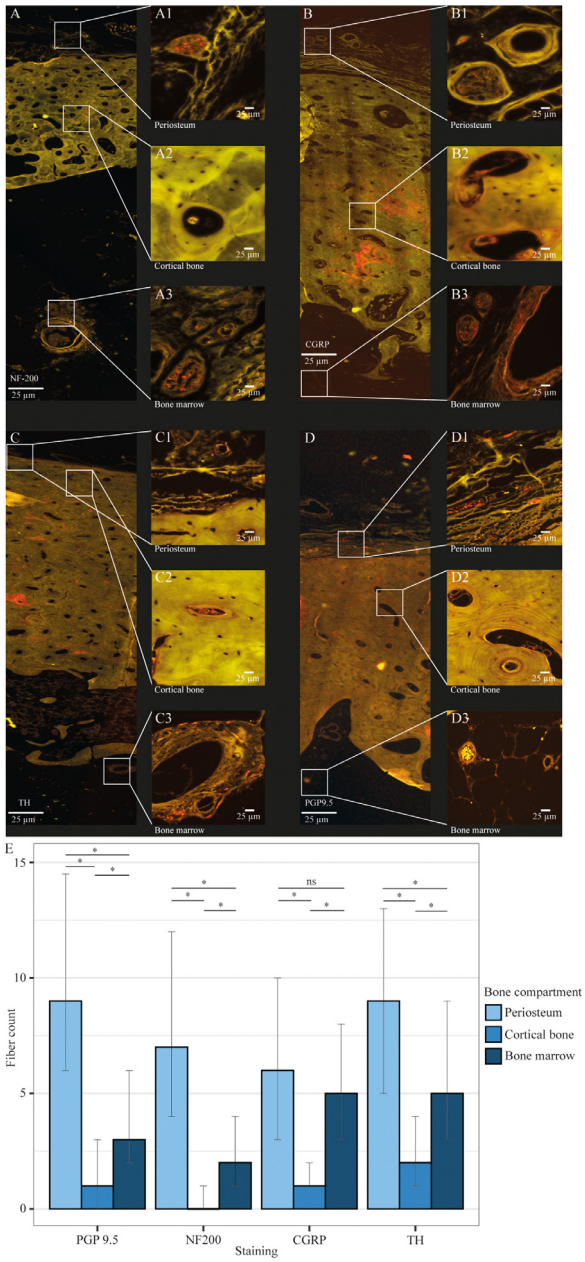

Figure 2. Fluorescent images showing NF-200-positive myelinated Aϑ-fibers (**A, A1-A3**), CGRP-positive unmyelinated C-fibers (**B, B1-B3**), TH-positive sympathetic nerve fibers (**C, C1-C3**), and PGP9.5-positive nerve fibers (**D, D1-D3**) in red. In periosteum and bone marrow, sensory nerve fibers were organized in large bundles (**A1**, **A3**, **B1**, **B3**), or were branched off as single nerve fibers (**A3**, **D1**). TH-positive sympathetic nerve fibers were co-localized with blood vessels (**C1**, **C3**). Cortical bone only contained sensory and sympathetic nerve fibers in Haversian canals (**C2**, **D2**), but not every canal was innervated (**A2**). Immunohistochemical stainings were quantified and presented as median (IQR) number of nerve fibers per HPF for periosteum (light blue), cortical bone (marine blue), and bone marrow (dark blue) (**E**). Fiber counts from all locations were combined. For every immunohistochemical staining, periosteum contained most nerve fibers, followed by the bone marrow, and cortical bone (color version of figure is available online.)

Nerve Fiber Distribution in Bone-Related Compartments

The periosteum and bone marrow cavity were innervated with large bundles of multiple sensory nerve

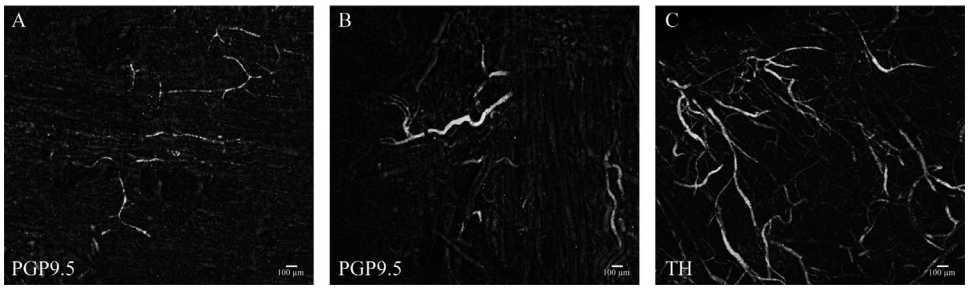

Figure 3. Confocal images of whole-mount preparations of periosteum from a radius (female, 83) demonstrating PGP9.5-positive nerve fibers (**A-B**), and TH-positive sympathetic nerve fibers (**C**) in white. PGP9.5-positive nerve fibers were organized in a branched network throughout the periosteum. TH-positive sympathetic nerve fibers were co-localized with blood vessels, which indirectly showed the abundancy of blood vessels in the periosteum.

fibers, while in the cortical bone only single fibers confined to Haversian canals were observed (Fig 2A1, A3, B1, D2 and 3A-3B). Sympathetic fibers were also present in all three bone-related compartments, but always co-localized with blood vessels (Fig 2C1-C3). Confocal images of periosteal whole-mount samples were prepared to allow assessment of coherence between nerve fibers, and illustrated that PGP9.5-positive nerve fibers (pan-neuronal marker) formed a branched network throughout the periosteum (Fig 3A-3B). Periosteal whole-mount preparations confirmed the co-localization of sympathetic fibers and blood vessels, and indirectly illustrated the abundancy of blood vessels in the periosteum (Fig 3C).

Differences between Aδ-fibers, C-fibers, and sympathetic nerve fibers within bone-related compartments were analyzed. See previous section and Fig 2E for median nerve fiber count. In periosteum, no difference between the number of Aδ-fibers and C-fibers was observed ($P = .71$). However, the number of C-fibers was significantly higher compared to the amount of Aδ-fibers in cortical bone, and bone marrow (both $P < .001$). Nerve fiber count for sympathetic nerve fibers was significantly higher compared with C-fibers in periosteum ($P < .001$). This difference was not observed in bone marrow or cortical bone ($P = 1.000$ and $P = .59$, respectively). The number of sympathetic nerve fibers was significantly higher compared with Aδ-fibers in cortical bone ($P < .001$), bone marrow ($P < .001$), and in periosteum ($P = .043$). These results indicate that in bone marrow and cortical bone, C-fibers are slightly more abundant than Aδ-fibers, while in periosteum both C-fibers and Aδ-fibers are present to the same extent. In addition, sympathetic fibers are large in number in every bone-related compartment.

Multivariate Regression

Possible effects of bone-related compartment, gender, age, anatomical location, and immunohistochemical staining on nerve fiber count were analyzed using a Poisson multivariate regression with interaction effects. Interaction tables and estimated marginal means (EMM) are provided in the supplementary information. The multivariate regression model was based on 1836 individual nerve fiber counts. In the elderly individuals studied (age range 66−99 years), the number of nerve fibers significantly declined per year of age (IRR = 0.985, $P < .001$), especially in the periosteum (Table 3, S1). No overall effect of sex on innervation density was present (male N = 738 counts, female N = 1098 counts, IRR = 1.016, $P = .881$), however the interaction effect between gender and anatomical location demonstrated higher nerve fiber counts for lower extremity bones of females (Table 3, S3, S8). The overall number of C-fibers was significantly lower compared to PGP9.5-positive nerve fibers (IRR = 0.650, $P = .003$) (Table 3, S2). No differences were observed in the number of Aδ-fibers (IRR = 1.225, $P = .132$) and sympathetic nerve fibers (IRR = 1.052, $P = .704$) compared to PGP9.5-positive nerve fibers (Table 3). The thoracic spine (IRR = 2.513, $P < .001$), upper extremity (IRR = 1.595, $P < .001$), and lower extremity (IRR = 1.540, $P < .001$) contained significantly more nerve fibers compared to neurocranium (Table 3, S5, S8, Fig 4). Nerve fiber count was significantly lower for bone marrow compared to periosteum (IRR = 0.189, $P < .001$), and lowest for cortical bone compared to periosteum (IRR = 0.094, $P < .001$). The low number of nerve fibers in cortical bone was mainly visible in female bones and lower extremity (Table S4, S7, S8).

Discussion

The present study set out to study the sensory innervation of human bone. The results demonstrate that the highest sensory innervation density can be found in the periosteum, followed by bone marrow and cortical bone. Of the locations studied, the thoracic vertebra received most sensory innervation. The neurocranium received the least sensory innervation. Innervation density decreased with age. In the present study, relative differences in innervation between periosteum, cortical bone and bone marrow were smaller compared to earlier mammalian studies.[8,37] One study reported a ratio of summed Aδ-fibers and C-fibers between periosteum, bone marrow and cortical bone of 100:2:0.1, while in the current study a ratio of 100:54:8 was found.[8] The use of a different species and calculations based on medians instead of means might partially account for these differences. Remarkably, not all osteons were innervated, which partially explained the low number of both sensory and sympathetic nerve fibers in cortical bone as presented in section 3.3 (Fig 2A2). The number

Table 3. Multivariate Regression Analyzing Factors that Influence Nerve Fiber Count Per High Power Field

Fiber count	*n=1836*	*GLM Poisson LogLink with interactions*				*GLM Poisson LogLink without interactions*			
		IRR	*EMM*,†*	*EMM SE*	P-*value*	*IRR*	*EMM*,†*	*EMM SE*	P-*value*
Intercept		25.153	4.32	0.080	**<.001**	23.871	4.42	0.073	**<.001**
Age	Per year	0.985	4.32	0.080	**<.001**	0.987	4.42	0.072	**<.001**
Gender	Male	*Reference*	4.32	0.114	N/A	*Reference*	3.97	0.084	N/A
	Female	1.016	4.33	0.112	.881	1.240	4.92	0.094	**<.001**
Staining	PGP9.5	*Reference*	4.88	0.151	N/A	*Reference*	5.47	0.118	N/A
	NF-200	1.225	2.78	0.125	.132	0.635	3.48	0.089	**<.001**
	CGRP	0.650	4.22	0.149	**.003**	0.706	3.86	0.097	**<.001**
	TH	1.052	6.11	0.181	.704	0.950	5.20	0.116	**<.001**
Location	Neurocranium	*Reference*	3.32	0.184	N/A	*Reference*	3.06	0.145	N/A
	Thoracic spine	2.513	5.73	0.191	**<.001**	2.057	6.28	0.163	**<.001**
	Upper extremity	1.595	4.83	0.123	**<.001**	1.567	4.79	0.103	**<.001**
	Lower extremity	1.540	3.81	0.072	**<.001**	1.359	4.15	0.065	**<.001**
Compartment	Periosteum	*Reference*	9.30	0.188	N/A	*Reference*	9.90	0.166	N/A
	Cortical bone	0.094	1.76	0.078	**<.001**	0.183	1.81	0.057	**<.001**
	Bone marrow	0.189	4.95	0.131	**<.001**	0.486	4.81	0.101	**<.001**

NOTE. All significant P-values are reported in bold.
*Results are averaged over the levels of other categorical variables. Estimated Marginal Means (EMM) represent the mean fiber count for each factor, adjusted for any other variables in the model. In the GLM Poisson LogLink without interactions, multiplying the factor's reference EMM (eg male in Gender) by the incident rate ratio (IRR) of non-reference categories gives the EMM for the non-reference category. Due to the involvement in interactions, this multiplication does not work in the GLM Poisson LogLink with interactions.
†Results may be misleading due to involvement in interactions

and distribution of sensory nerve fibers varied between different anatomical locations (ie neurocranium, thoracic spine, upper, and lower extremity). Possibly, skeletal injury in more densely innervated locations is more painful than in locations receiving less sensory innervation. Previous reports have shown correlations between innervation of the intervertebral disc and severity of low back pain. However, a causal relationship between innervation density and pain severity cannot be established, as tissue injury (inflicting pain) and the subsequent inflammatory processes have been shown to lead to hyperinnervation.[1] Gerbershagen *et al.* studied pain scores on the first postoperative day for any type of surgery. The top ten of most painful interventions included seven skeletal surgeries, of which three were in the spinal column.[18] Although pain is a multidimensional phenomenon and not necessarily equal to sensory innervation density, the high nerve fiber count in thoracic spine as demonstrated in the current study reflects these clinical findings, supporting a correlation between innervation density and pain severity.

We demonstrated that sensory nerve fibers in periosteum were organized in a network of large bundles or were branched off as single nerve fibers forming a net-like structure. The typical symptom of a bone fracture is acute, stabbing pain localized near or at the fracture site.[52] Mechanical distortion of the periosteum might help explain the severe pain experienced by these patients. In addition, skeletal pain can be caused by pathology in the bone marrow (eg in bone tumors), and is typically described as a dull and aching pain.[22,35,45,46] In the present study we demonstrated that the number of C-fibers was slightly higher compared to the number of Aδ-fibers in bone marrow. This finding is in line with the clinical picture of patients experiencing different types of pain in different types of pathology. The here presented data may provide new treatment targets for these various types of pain arising from skeletal pathology.

A strength of this study was the use of four immunohistochemical stains to visualize Aδ-fibers, C-fibers, and sympathetic fibers. Subsequently, we were able to draw conclusions about their relative number in different bone-related compartments. It should be noted that the total volume of bone marrow is greater than cortical bone and periosteum.[37] Therefore, the absolute number of sensory and sympathetic nerve fibers might be higher in bone marrow. Use of multivariate regression enabled us to draw conclusions on the complete data set. For example, to analyze the effect of gender on bone innervation, all 1836 observations were taken into account. Another strong element of the present study was the use of bones from multiple anatomical locations, to adequately represent human axial and appendicular innervation. The use of bones from both men and women of ages ranging from 66 to 99 were used to account for potential differences in bone innervation based on sex or age. Our findings demonstrated no overall differences in innervation between female and male bones. Collecting all four bone sites studied from the same individual would have provided paired samples and thus might have further strengthened our conclusions, but was not possible due to incompleteness of the skeletal material available. Furthermore, experiments were performed on macroscopically healthy bones, making the results relevant to the general population. As mentioned, average donor age was relatively high (84 ± 8.2 y) and ranged from 66 until 99 years. We found that the number of sensory and sympathetic

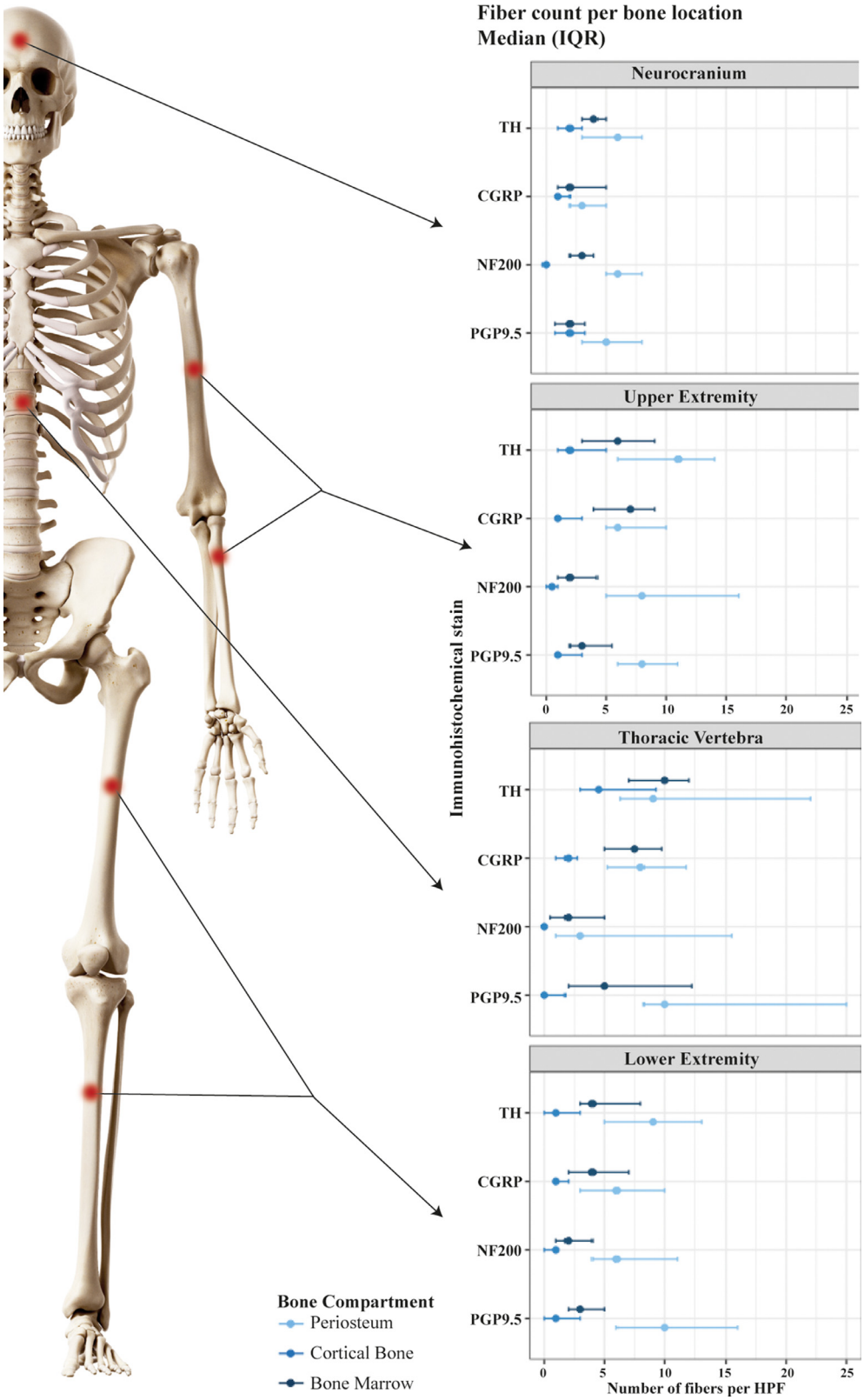

Figure 4. The median number (IQR) of CGRP-positive unmyelinated C-fibers, NF-200-positive myelinated A∂-fibers, TH-positive sympathetic nerve fibers, and PGP9.5-positive nerve fibers separately displayed for the neurocranium, thoracic vertebra, upper extremity, and lower extremity. Compared to the neurocranium, the number of nerve fibers was higher in all three anatomical locations, especially in the thoracic vertebra. Skeleton adjusted from sciepro/shutterstock.com, used under license of Shutterstock.com.

nerve fibers declined with age, which is consistent with a previous animal study.[9] Nevertheless, a wider age range of subjects is necessary to determine whether our findings are applicable for a younger population. A drawback of using anonymous human cadavers, is that the cause of death and its possible effects on bone innervation remains unknown. Previous studies on human innervation have reported on the effects of

osteoarthritis and degenerative disc disease on bone innervation. To avoid influence of joint diseases on nerve fiber density, we collected samples from midshaft regions of bone only.[6,28] CGRP-positive fibers have been reported to have a punctuated morphology, while the NF200 signal has a continuous morphology. To avoid overestimation of CGRP-positive fibers due to their morphology, bone cross-sections were used for nerve fiber quantification. As nerve fibers run parallel to the longitudinal axis of long bones, risks of overcounting are minimized. Another possible limitation is the increased EDTA bone decalcification time when compared to previously conducted mammalian studies (>3 wk vs 2 wk).[8,9,37] The extended decalcification was necessary to demineralize cortical bone, which is thicker in humans than in rodents. Literature described that EDTA negatively affects the antigenicity of A∂-fibers, C-fibers, and sympathetic fibers.[9,37] This might have resulted in a lower nerve fiber count in the present study and thus underestimation of overall innervation density, although this is expected to equally affect all bone compartments and thus does not necessarily impact the here presented ratios. Contradictory reports on the effect of formaldehyde on immunoreactivity of tissue exist.[3,57] The specimens have been fixated in formaldehyde for various amounts of time, which might have led to variation in immunoreactivity. Our and others' experience is that no large differences regarding immunoreactivity between fresh-frozen samples and formaldehyde-fixated samples were present.[57] Fourth, since PGP9.5 is a pan-neuronal marker, the number of PGP9.5-positive nerve fibers should theoretically equal the sum of A∂-fibers, C-fibers, and sympathetic fibers. However, in the present study we found that the sum of A∂-fibers, C-fibers, and sympathetic fibers was approximately 4 times the number of PGP9.5-positive nerve fibers in bone marrow. For periosteum and cortical bone, similar computations resulted in a factorial difference of about 2.4 and 3, respectively. This finding was remarkable as previous studies reported adequate specificity of the immunohistochemical markers used, and showed a lack of other sensory nerve fibers innervating the bone such as Aβ-fibers.[4,20,24,30,51,64] Although CGRP has been used as a marker for non-myelinated fibers in similar experiments,[16,37] other studies have shown CGRP to be expressed by A∂-fibers.[25] Further, calculations with median nerve fiber counts and usage of separate microscopic slides for each neuronal marker might have contributed to this discrepancy. These factors might explain the observation that the sum of A∂-fibers, C-fibers, and sympathetic fibers exceeded PGP9.5 fiber count and highlights the need for a more specific C-fiber marker. However, as these limitations were present in all bones and bone compartments, the authors suggest that these phenomena do not affect the overall trends observed in this study nor the final conclusions.

Conclusion

To our knowledge, the present study is the first to demonstrate the sensory innervation in the human axial and appendicular skeleton. The current results provide an explanation for the severe pain experienced by patients suffering from musculoskeletal diseases or following skeletal surgery. The number of sensory and sympathetic nerve fibers was highest in periosteum, followed by bone marrow and cortical bone. Of all locations studied, bone from thoracic vertebral bodies was most densely innervated. In the periosteum, sensory nerve fibers were organized in a net-like structure that may allow for detection of mechanical distortion such as experienced during traumatic events. The number of nerve fibers declined with age. Since the periosteum is the most densely innervated bone-related compartment in human bones, treatment strategies that locally target the periosteum might aid in attenuating pain after skeletal surgery. Future studies are needed to understand how bone diseases affect density, sensitivity, and morphology of sensory and sympathetic nerve fibers.

Acknowledgments

We would like to thank prof. dr. Ronald Bleys, Simon Plomp, and Marco Rondhuis from the Department of Anatomy (UMC Utrecht) for their help with tissue collection, designing immunohistochemical protocols, and for using their microscope facility. Peter Zuithoff from the Julius Center (Utrecht) is thanked for valuable input on statistical analysis. The Developmental Studies Hybridoma Bank is gratefully acknowledged for supplying the NF-200 antibody. No financial arrangements that may represent a possible conflict of interest are present. The authors declare that they have no conflict of interest.

For the purpose of replicating procedures and reproducing results, data and program codes are available upon request. Requests can be sent to the corresponding author.

Supplementary data

Supplementary data related to this article can be found at https://doi.org/10.1016/j.jpain.2021.04.006.

References

1. Amaya F, Izumi Y, Matsuda M, Sasaki M: Tissue injury and related mediators of pain exacerbation. Curr Neuropharmacol 11:592-597, 2013

2. Bataille C, Mauprivez C, Hay E, Baroukh B, Brun A, Chaussain C, Marie PJ, Saffar J-L, Cherruau M: Different sympathetic pathways control the metabolism of distinct bone envelopes. Bone 50:1162-1172, 2012

3. Benerini Gatta L, Cadei M, Balzarini P, Castriciano S, Paroni R, Verzeletti A, Cortellini V, De Ferrari F, Grigolato P: Application of alternative fixatives to formalin in diagnostic pathology. Eur J Histochem 56:e12, 2012

4. Bernal Sierra YA, Haseleu J, Kozlenkov A, Begay V, Lewin GR: Genetic tracing of Cav3.2 T-type calcium channel expression in the peripheral nervous system. Front Mol Neurosci 10:70, 2017

5. Brooks PM: The burden of musculoskeletal disease—a global perspective. Clin Rheumatol 25:778-781, 2006

6. Brown MF, Hukkanen M V, McCarthy ID, Redfern DR, Batten JJ, Crock H V, Hughes SP, Polak JM: Sensory and sympathetic innervation of the vertebral endplate in patients with degenerative disc disease. J Bone Joint Surg Br 79:147-153, 1997

7. Cao J, Zhang S, Gupta A, Du Z, Lei D, Wang L, Wang X: Sensory nerves affect bone regeneration in rabbit mandibular distraction osteogenesis. Int J Med Sci 16:831-837, 2019

8. Castaneda-Corral G, Jimenez-Andrade JM, Bloom AP, Taylor RN, Mantyh WG, Kaczmarska MJ, Ghilardi JR, Mantyh PW: The majority of myelinated and unmyelinated sensory nerve fibers that innervate bone express the tropomyosin receptor kinase A. Neuroscience 178:196-207, 2011

9. Chartier SR, Mitchell SAT, Majuta LA, Mantyh PW: The changing sensory and sympathetic innervation of the young, adult and aging mouse femur. Neuroscience 387:178-190, 2018

10. Chartier SR, Thompson ML, Longo G, Fealk MN, Majuta LA, Mantyh PW: Exuberant sprouting of sensory and sympathetic nerve fibers in nonhealed bone fractures and the generation and maintenance of chronic skeletal pain. Pain 155:2323-2336, 2014

11. Chen L-J, Zhang F-G, Li J, Song H-X, Zhou L-B, Yao B-C, Li F, Li W-C: Expression of calcitonin gene-related peptide in anterior and posterior horns of the spinal cord after brachial plexus injury. J Clin Neurosci Off J Neurosurg Soc Australas Scotland 17:87-91, 2010

12. Cimmino MA, Ferrone C, Cutolo M: Epidemiology of chronic musculoskeletal pain. Best Pract Res Clin Rheumatol Netherlands 25:173-183, 2011

13. Dominick KL, Ahern FM, Gold CH, Heller DA: Health-related quality of life and health service use among older adults with osteoarthritis. Arthritis Rheum United States 51:326-331, 2004

14. Doran JF, Jackson P, Kynoch PA, Thompson RJ: Isolation of PGP 9.5, a new human neurone-specific protein detected by high-resolution two-dimensional electrophoresis. J Neurochem 40:1542-1547, 1983

15. Edgar MA: The nerve supply of the lumbar intervertebral disc. J Bone Joint Surg Br 89:1135-1139, 2007

16. Eftekhari S, Warfvinge K, Blixt FW, Edvinsson L: Differentiation of nerve fibers storing CGRP and CGRP receptors in the peripheral trigeminovascular system. J pain 14:1289-1303, 2013

17. Eimar H, Tamimi I, Murshed M, Tamimi F: Cholinergic regulation of bone. J Musculoskelet Neuron 13:124-132, 2013

18. Gerbershagen HJ, Aduckathil S, van Wijck AJM, Peelen LM, Kalkman CJ, Meissner W: Pain intensity on the first day after surgery: a prospective cohort study comparing 179 surgical procedures. Anesthesiology 118:934-944, 2013

19. Gervasi NM, Scott SS, Aschrafi A, Gale J, Vohra SN, MacGibeny MA, Kar AN, Gioio AE, Kaplan BB: The local expression and trafficking of tyrosine hydroxylase mRNA in the axons of sympathetic neurons. RNA 22:883-895, 2016

20. Haskins W, Benitez S, Mercado JM, Acosta CG: Cutaneous inflammation regulates THIK1 expression in small C-like nociceptor dorsal root ganglion neurons. Mol Cell Neurosci 83:13-26, 2017

21. Hoy D, Bain C, Williams G, March L, Brooks P, Blyth F, Woolf A, Vos T, Buchbinder R: A systematic review of the global prevalence of low back pain. Arthritis Rheum 64:2028-2037, 2012

22. Ivanusic JJ: Molecular mechanisms that contribute to bone marrow pain. Front Neurol 8:458, 2017

23. Ivanusic JJ: Size, neurochemistry, and segmental distribution of sensory neurons innervating the rat tibia. J Comp Neurol 517:276-283, 2009

24. Ivanusic JJ, Mahns DA, Sahai V, Rowe MJ: Absence of large-diameter sensory fibres in a nerve to the cat humerus. J Anat 208:251-255, 2006

25. Iyengar S, Ossipov MH, Johnson KW: The role of calcitonin gene-related peptide in peripheral and central pain mechanisms including migraine. Pain 158:543-559, 2017

26. Jimenez-Andrade JM, Bloom AP, Mantyh WG, Koewler NJ, Freeman KT, Delong D, Ghilardi JR, Kuskowski MA, Mantyh PW: Capsaicin-sensitive sensory nerve fibers contribute to the generation and maintenance of skeletal fracture pain. Neuroscience 162:1244-1254, 2009

27. Jimenez-Andrade JM, Mantyh WG, Bloom AP, Xu H, Ferng AS, Dussor G, Vanderah TW, Mantyh PW: A phenotypically restricted set of primary afferent nerve fibers innervate the bone versus skin: therapeutic opportunity for treating skeletal pain. Bone 46:306-313, 2010

28. Koeck FX, Schmitt M, Baier C, Stangl H, Beckmann J, Grifka J, Straub RH: Predominance of synovial sensory nerve fibers in arthrofibrosis following total knee arthroplasty compared to osteoarthritis of the knee. J Orthop Surg Res 11:25, 2016

29. Koo TK, Li MY: A guideline of selecting and reporting intraclass correlation coefficients for reliability research. J Chiropr Med 15:155-163, 2016

30. Lawson SN, Perry MJ, Prabhakar E, McCarthy PW: Primary sensory neurones: neurofilament, neuropeptides, and conduction velocity. Brain Res Bull 30:239-243, 1993

31. Lawson SN, Waddell PJ: Soma neurofilament immunoreactivity is related to cell size and fibre conduction velocity in rat primary sensory neurons. J Physiol 435:41-63, 1991

32. Leigh JP, Seavey W, Leistikow B: Estimating the costs of job related arthritis. J Rheumatol 28:1647-1654, 2001

33. Longo G, Osikowicz M, Ribeiro-da-Silva A: Sympathetic fiber sprouting in inflamed joints and adjacent skin contributes to pain-related behavior in arthritis. J Neurosci United States; 33:10066-10074, 2013

34. Lubeck DP: The costs of musculoskeletal disease: health needs assessment and health economics. Best Pract Res Clin Rheumatol 17:529-539, 2003

35. Luger NM, Mach DB, Sevcik MA, Mantyh PW: Bone cancer pain: from model to mechanism to therapy. J Pain Symptom Manage 29:S32-S46, 2005

36. Lundberg LM, Alm P, Wharton J, Polak JM: Protein gene product 9.5 (PGP 9.5). A new neuronal marker visualizing the whole uterine innervation and pregnancy-induced and developmental changes in the guinea pig. Histochemistry 90:9-17, 1988

37. Mach DB, Rogers SD, Sabino MC, Luger NM, Schwei MJ, Pomonis JD, Keyser CP, Clohisy DR, Adams DJ, O'leary P, Mantyh PW: Origins of skeletal pain: Sensory and sympathetic innervation of the mouse femur. Neuroscience 113:155-166, 2002

38. Mahns DA, Ivanusic JJ, Sahai V, Rowe MJ: An intact peripheral nerve preparation for monitoring the activity of single, periosteal afferent nerve fibres. J Neurosci Methods 156:140-144, 2006. 2006/03/30. Netherlands

39. Mantyh PW: Mechanisms that drive bone pain across the lifespan. Br J Clin Pharmacol 85:1103-1113, 2019

40. Mantyh PW: The neurobiology of skeletal pain. Eur J Neurosci 39:508-519, 2014

41. Martin CD, Jimenez-Andrade JM, Ghilardi JR, Mantyh PW: Organization of a unique net-like meshwork of CGRP+ sensory fibers in the mouse periosteum: implications for the generation and maintenance of bone fracture pain. Neurosci Lett 427:148-152, 2007

42. McCarthy EF: Genetic diseases of bones and joints. Semin Diagn Pathol 28:26-36, 2011

43. Miyagi M, Millecamps M, Danco AT, Ohtori S, Takahashi K, Stone LS: ISSLS Prize winner: Increased innervation and sensory nervous system plasticity in a mouse model of low back pain due to intervertebral disc degeneration. Spine 39:1345-1354, 2014

44. Murray CJL, Lopez AD, Organization WH, Bank W, Health HS of P: The Global burden of disease : a comprehensive assessment of mortality and disability from diseases, injuries, and risk factors in 1990 and projected to 2020 : summary /edited by Christopher J.L. Murray, Alan D. Lopez. Geneva PP - Geneva: World Health Organization; 1996.

45. Nencini S, Ivanusic J: Mechanically sensitive Adelta nociceptors that innervate bone marrow respond to changes in intra-osseous pressure. J Physiol 595:4399-4415, 2017

46. Nencini S, Ivanusic JJ: The physiology of bone pain. How much do we really know? Front Physiol 7:157, 2016

47. Nencini S, Ringuet M, Kim D-H, Chen Y-J, Greenhill C, Ivanusic JJ: Mechanisms of nerve growth factor signaling in bone nociceptors and in an animal model of inflammatory bone pain. Mol Pain 13:1744806917697011, 2017

48. Oostinga D, Steverink JG, van Wijck AJM, Verlaan J-J: An understanding of bone pain: A narrative review. Bone 134:115272, 2020

49. Ralston HJ, Miller MR, Kasahara M: Nerve endings in human fasciae, tendons, ligaments, periosteum, and joint synovial membrane. Anat Rec 136:137-147, 1960

50. Rosemann T, Laux G, Kuehlein T: Osteoarthritis and functional disability: results of a cross sectional study among primary care patients in Germany. BMC Musculoskelet Disord 8:79, 2007

51. Rots ML, de Borst GJ, van der Toorn A, Moll FL, Pennekamp CWA, Dijkhuizen RM, Bleys RLAW: Effect of bilateral carotid occlusion on cerebral hemodynamics and perivascular innervation: An experimental rat model. J Comp Neurol 527:2263-2272, 2019

52. Santy J, Mackintosh C: A phenomenological study of pain following fractured shaft of femur. J Clin Nurs 10:521-527, 2001

53. Sawatzky R, Liu-Ambrose T, Miller WC, Marra CA: Physical activity as a mediator of the impact of chronic conditions on quality of life in older adults. Health Qual Life Outcomes 5:68, 2007

54. Sayilekshmy M, Hansen RB, Delaissé J-M, Rolighed L, Andersen TL, Heegaard A-M: Innervation is higher above Bone Remodeling Surfaces and in Cortical Pores in Human Bone: Lessons from patients with primary hyperparathyroidism. Sci Rep Nat 9:5361, 2019

55. Schober P, Boer C, Schwarte LA: Correlation coefficients: Appropriate use and interpretation. Anesth Analg 126:1763-1768, 2018

56. Schou WS, Ashina S, Amin FM, Goadsby PJ, Ashina M: Calcitonin gene-related peptide and pain: A systematic review. J Headache Pain 18:34, 2017

57. Shi S-R, Liu C, Pootrakul L, Tang L, Young A, Chen R, Cote RJ, Taylor CR: Evaluation of the value of frozen tissue section used as "gold standard" for immunohistochemistry. Am J Clin Pathol 129:358-366, 2008

58. St Sauver JL, Warner DO, Yawn BP, Jacobson DJ, McGree ME, Pankratz JJ, Melton LJ 3rd, Roger VL, Ebbert JO, Rocca WA: Why patients visit their doctors: assessing the most prevalent conditions in a defined American population. Mayo Clin Proc 88:56-67, 2013

59. Thai J, Kyloh M, Travis L, Spencer NJ, Ivanusic JJ: Identifying spinal afferent (sensory) nerve endings that innervate the marrow cavity and periosteum using anterograde tracing. J Comp Neurol, 2020. https://doi.org/10.1002/cne.24862

60. Thompson RJ, Doran JF, Jackson P, Dhillon AP: Rode J: PGP 9.5—a new marker for vertebrate neurons and neuroendocrine cells. Brain Res 278:224-228, 1983

61. Thurston TJ: Distribution of nerves in long bones as shown by silver impregnation. J Anat 134:719-728, 1982

62. Woolf AD, Erwin J, March L: The need to address the burden of musculoskeletal conditions. Best Pract Res Clin Rheumatol 26:183-224, 2012

63. Woolf AD, Pfleger B: Burden of major musculoskeletal conditions. Bull World Health Organ 81:646-656, 2003

64. Yen LD, Bennett GJ, Ribeiro-da-Silva A: Sympathetic sprouting and changes in nociceptive sensory innervation in the glabrous skin of the rat hind paw following partial peripheral nerve injury. J Comp Neurol 495:679-690, 2006